Research Article | Vol. 26, No. 10 | 14 May 2018 | OPTICS EXPRESS 13666
Optics EXPRESS

Controlling nonsequential double ionization of Ne with parallel-polarized two-color laser pulses

SIQIANG LUO,[1,3] XIAOMENG MA,[1,3] HUI XIE,[1] MIN LI,[1,*] YUEMING ZHOU,[1,4] WEI CAO,[1] AND PEIXIANG LU[1,2]

[1] *Wuhan National Laboratory for Optoelectronics and School of Physics, Huazhong University of Science and Technology, Wuhan 430074, China*
[2] *Laboratory of Optical Information Technology, Wuhan Institute of Technology, Wuhan 430205, China*
[3] *These authors contributed equally to this work*
[4] *zhouymhust@hust.edu.cn*
[*] *mli@hust.edu.cn*

Abstract: We measure the recoil-ion momentum distributions from nonsequential double ionization of Ne by two-color laser pulses consisting of a strong 800-nm field and a weak 400-nm field with parallel polarizations. The ion momentum spectra show pronounced asymmetries in the emission direction, which depend sensitively on the relative phase of the two-color components. Moreover, the peak of the doubly charged ion momentum distribution shifts gradually with the relative phase. The shifted range is much larger than the maximal vector potential of the 400-nm laser field. Those features are well recaptured by a semiclassical model. Through analyzing the correlated electron dynamics, we found that the energy sharing between the two electrons is extremely unequal at the instant of recollison. We further show that the shift of the ion momentum corresponds to the change of the recollision time in the two-color laser field. By tuning the relative phase of the two-color components, the recollision time is controlled with attosecond precision.

OCIS codes: (020.4180) Multiphoton processes; (260.3230) Ionization;(270.6620) Strong-field processes.

References and links

1. P. B. Corkum, "Plasma perspective on strong field multiphoton ionization," Phys. Rev. Lett. **71**(13), 1994–1997(1993).
2. A. McPherson, G. Gibson, H. Jara, U. Johann, T. S. Luk, I. A. McIntyre, K. Boyer, and C. K. Rhodes, "Studies of multiphoton production of vacuum-ultraviolet radiation in the rare gases," J. Opt. Soc. Am. B **4**(4), 595–601 (1987).
3. M. Ferray, A. L'Huillier, X. F. Li, L. A. Lompré, G. Mainfray and C. Manus, "Multiple-harmonic conversion of 1064 nm radiation in rare gases," J. Phys. B **21**(3), L31 (1988).
4. B. Wang, L. He, F. Wang, H. Yuan, X. Zhu, P. Lan, and P. Lu, "Resonance-modulated wavelength scaling of high-order-harmonic generation from H_2^+," Phys. Rev. A **97**(1), 013417 (2018).
5. C. Zhai, X. Zhang, X. Zhu, L. He, Y. Zhang, B. Wang, Q. Zhang, P. Lan, and P. Lu, "Single-shot molecular orbital tomography with orthogonal two-color fields," Opt. Express **26**(3), 2775–2784 (2018).
6. L. He, Q. Zhang, P. Lan, W. Cao, X. Zhu, C. Zhai, F. Wang, W. Shi, M. Li, X. Bian, P. Lu and André D. Bandrauk, "Monitoring ultrafast vibrational dynamics of isotopic molecules with frequency modulation of high-order harmonics," Nat. Commun. **9**(1), 1108 (2018).
7. M. He, Y. Li, Y. Zhou, M. Li, W. Cao, and P. Lu, "Direct Visualization of Valence Electron Motion Using Strong-Field Photoelectron Holography," Phys. Rev. Lett. **120**(13), 133204 (2018).
8. W. Becker, F. Grasbon, R. Kopold, D. Milošević, G. Paulus, and H. Walther, "Above-threshold ionization: From classical features to quantum effects," Adv. At. Mol. Opt. Phys. **48**, 35–98 (2002).
9. J. Tan, Yang Li, Y. Zhou, M. He, Y. Chen, M. Li, P. Lu, "Identifying the contributions of multiple-returning recollision orbits in strong-field above-threshold ionization," Opt. Quant. Electron. **50**(2), 57 (2018).
10. B. Wolter, M. G. Pullen, A.-T. Le, M. Baudisch, K. Doblhoff-Dier, A. Senftleben, M. Hemmer, C. D. Schröter, J. Ullrich, T. Pfeifer, R. Moshammer, S. Gräfe, O. Vendrell, C. D. Lin and J. Biegert, " Ultrafast electron diffraction imaging of bond breaking in di-ionized acetylene," Science **354**(6310), 308 (2016).
11. M. G. Pullen, B. Wolter, A. -T. Le, M. Baudisch, M. Hemmer, A. Senftleben, C. D. Schröter, J. Ullrich, R. Moshammer, C. D. Lin and J. Biegert, " Imaging an aligned polyatomic molecule with laser-induced electron diffraction," Nat. Commun. **6**(1), 7262 (2015).
12. M. G. Pullen, B. Wolter, A. -T. Le, M. Baudisch, M. Sclafani, H. Pires, C. D. Schröter, J. Ullrich, R. Moshammer, T. Pfeifer, C. D. Lin and J. Biegert, " Influence of orbital symmetry on diffraction imaging with rescattering electron

#327200 https://doi.org/10.1364/OE.26.013666
Journal © 2018 Received 28 Mar 2018; revised 3 May 2018; accepted 3 May 2018; published 11 May 2018

Optics EXPRESS

wave packets," Nat. Commun. **7**, 11922 (2016).
13. D. N. Fittinghoff, P. R. Bolton, B. Chang, and K. C. Kulander, "Observation of nonsequential double ionization of helium with optical tunneling," Phys. Rev. Lett. **69**(18), 2642–2645 (1992).
14. B. Walker, B. Sheehy, L.F. DiMauro, P. Agostini, K.J. Schafer, and K. C. Kulander, "Precision measurement of strong field double ionization of helium," Phys. Rev. Lett. **73**(9), 1227–1230 (1994).
15. Th. Weber, H. Giessen, M. Weckenbrock, G. Urbasch, A. Staudte, L. Spielberger, O. Jagutzki, V. Mergel, M. Vollmer, and R. Dörner, "Correlated electron emission in multiphoton double ionization," Nature (London) **405**(6787), 658–661 (2000).
16. R. Moshammer, J. Ullrich, B. Feuerstein, D. Fischer, A. Dorn, C. D. Schröter, J. R. Crespo López-Urrutia, C. Höhr, H. Rottke, C. Trump, M. Wittmann, G. Korn, K. Hoffmann, and W. Sandner, "Strongly directed electron emission in non-sequential double ionization of Ne by intense laser pulses," J. Phys. B **36**(6), L113 (2003).
17. M. Weckenbrock, D. Zeidler, A. Staudte, Th. Weber, M. Schöffler, M. Meckel, S. Kammer, M. Smolarski, O. Jagutzki, V. R. Bhardwaj, D. M. Rayner, D. M. Villeneuve, P. B. Corkum, and R. Dörner, "Fully Differential Rates for Femtosecond Multiphoton Double Ionization of Neon," Phys. Rev. Lett. **92**(21), 213002 (2004).
18. Y. Liu, S. Tschuch, A. Rudenko, M. Dürr, M. Siegel, U. Morgner, R. Moshammer, and J. Ullrich, "Strong-Field Double Ionization of Ar below the Recollision Threshold," Phys. Rev. Lett. **101**(5), 053001 (2008).
19. A. Rudenko, V. L. B. de Jesus, Th. Ergler, K. Zrost, B. Feuerstein, C. D. Schröter, R. Moshammer, and J. Ullrich, "Correlated Two-Electron Momentum Spectra for Strong-Field Nonsequential Double Ionization of He at 800 nm," Phys. Rev. Lett. **99**(26), 263003 (2007).
20. A. Staudte, C. Ruiz, M. Schöffler, S. Schössler, D. Zeidler, Th. Weber, M. Meckel, D. M. Villeneuve,P. B. Corkum, A. Becker, and R. Dörner, "Binary and Recoil Collisions in Strong Field Double Ionization of Helium," Phys. Rev. Lett. **99**(26), 263002 (2007).
21. Y. Liu, L. Fu, D. Ye, J. Liu, M. Li, C. Wu, Q. Gong, R. Moshammer, and J. Ullrich, "Strong-Field Double Ionization through Sequential Release from Double Excitation with Subsequent Coulomb Scattering," Phys. Rev. Lett. **112**(1), 013003 (2014).
22. C. Ruiz and A. Becker, "Time-resolved mapping of correlated electron emission from helium atom in an intense laser pulse," New J. Phys. **10**(2), 025020 (2008).
23. Y. Chen, Y. Zhou, Y. Li, M. Li, P. Lan, and P. Lu, "Rabi oscillation in few-photon double ionization through doubly excited states," Phys. Rev. A **97**(1), 013428 (2018).
24. N. Li, Y. Zhou, X. Ma, M. Li, C. Huang, and P. Lu, "Correlated electron dynamics in strong-field nonsequential double ionization of Mg," J. Chem. Phys. **147**(17), 174302 (2017).
25. B. Feuerstein, R. Moshammer, D. Fischer, A. Dorn, C. D. Schröter, J. Deipenwisch, J. R. Crespo López-Urrutia, C. Höhr, P. Neumayer, J. Ullrich, H. Rottke, C. Trump, M. Wittmann, G. Korn, and W. Sandner, "Separation of Recollision Mechanisms in Nonsequential Strong Field Double Ionization of Ar: The Role of Excitation Tunneling," Phys. Rev. Lett. **87**(4), 043003 (2001).
26. D. Ye, M. Li, L. Fu, J. Liu, Q. Gong, Y. Liu, and J. Ullrich, "Scaling Laws of the Two-Electron Sum-Energy Spectrum in Strong-Field Double Ionization," Phys. Rev. Lett. **115**(12), 123001 (2015).
27. X. Ma, Y. Zhou, P. Lu, "Multiple recollisions in strong-field nonsequential double ionization," Phys. Rev. A **93**(1), 013425 (2016).
28. C. Huang, M. Zhong, and Z. Wu, "Recollision dynamics in nonsequential double ionization of atoms by long-wavelength pulses," Opt. Express **24**(25), 28361–28371 (2016).
29. X. Ma, M. Li, Y. Zhou, P. Lu, "Nonsequential double ionization of Xe by mid-infrared laser pulses," Opt. Quant. Electron **49**(4), 170 (2017).
30. F. Krausz and M. Ivanov, "Attosecond physics," Rev. Mod. Phys. **81**(1), 163–234 (2009).
31. X. Liu, and C. Figueira de Morisson Faria, "Nonsequential Double Ionization with Few-Cycle Laser Pulses," Phys. Rev. Lett. **92**(13), 133006 (2004).
32. N. Johnson, O. Herrwerth, A. Wirth, S. De, I. Ben-Itzhak, M. Lezius, B. Bergues, M. F. Kling, A. Senftleben, C. D. Schröter, R. Moshammer, J. Ullrich, K. J. Betsch, R. R. Jones, A. M. Sayler, T. Rathje, K. Rühle, W. Müller, and G. G. Paulus, "Single-shot carrier-envelope-phase-tagged ion-momentum imaging of nonsequential double ionization of argon in intense 4-fs laser fields," Phys. Rev. A **83**(1), 013412 (2011).
33. X. Liu, H. Rottke, E. Eremina, W. Sandner, E. Goulielmakis, K. O. Keeffe, M. Lezius, F. Krausz, F. Lindner, M. G. Schätzel, G. G. Paulus, and H. Walther, "Nonsequential Double Ionization at the Single-Optical-Cycle Limit," Phys. Rev. Lett. **93**(26), 263001 (2004).
34. G. Xin, D. Ye, and J. Liu, "Dependence of the correlated-momentum patterns in double ionization on the carrier-envelope phase and intensity of a few-cycle laser pulse," Phys. Rev. A **82**(6), 063423 (2010).
35. B. Bergues, M. Kübel, Nora. G. Johnson, B. Fischer, N. Camus, K. J. Betsch, O. Herrwerth, A. Senftleben, A. Max Sayler, T. Rathje, T. Pfeifer, I. Ben-Itzhak, R. R. Jones, G. G. Paulus, F. Krausz, R. Moshammer, J. Ullrich, and M. F. Kling, "Attosecond tracing of correlated electron-emission in non-sequential double ionization," Nat. Commun. **3**(3), 813 (2012).
36. N. Camus, B. Fischer, M. Kremer, V. Sharma, A. Rudenko, B. Bergues, M. Kübel, N. G. Johnson, M. F. Kling, T. Pfeifer, J. Ullrich, and R. Moshammer, "Attosecond Correlated Dynamics of Two Electrons Passing through a Transition State," Phys. Rev. Lett. **108**(7), 073003 (2012).
37. M. Kübel, Nora G. Kling, K. J. Betsch, N. Camus, A. Kaldun, U. Kleineberg, I. Ben-Itzhak, R. R. Jones, G. G. Paulus,

Optics EXPRESS

T. Pfeifer, J. Ullrich, R. Moshammer, M. F. Kling, and B. Bergues, "Nonsequential double ionization of N_2 in a near-single-cycle laser pulse," Phys. Rev. A **88**(2), 023418 (2013).
38. Y. Zhou, C. Huang, A. Tong, Q. Liao, and P. Lu, "Correlated electron dynamics in nonsequential double ionization by orthogonal two-color laser pulses," Opt. Express **19**(3), 2301–2308 (2011).
39. L. Chen, Y. Zhou, C. Huang, Q. Zhang, and P. Lu, "Attosecond-resolved electron emission in nonsequential double ionization," Phys. Rev. A **88**(4), 043425 (2013).
40. Z. Yuan, D. Ye, Q. Xia, J. Liu, and L. Fu, "Intensity-dependent two-electron emission dynamics with orthogonally polarized two-color laser fields," Phys. Rev. A **91**(6), 063417 (2015).
41. L. Zhang, X. Xie, S. Roither, Y. Zhou, P. Lu, D. Kartashov, M. Schöffler, D. Shafir, P. B. Corkum, A. Baltuška, A. Staudte, and M. Kitzler, "Subcycle control of electron-electron correlation in double ionization," Phys. Rev. Lett. **112**(19), 193002 (2014).
42. Jan L. Chaloupka and Daniel D. Hickstein, "Dynamics of Strong-Field Double Ionization in Two-Color Counterrotating Fields," Phys. Rev. Lett. **116**(14), 143005 (2016).
43. Christopher A. Mancuso, Kevin M. Dorney, Daniel D. Hickstein, Jan L. Chaloupka, Jennifer L. Ellis, Franklin J. Dollar, Ronny Knut, Patrik Grychtol, Dmitriy Zusin, Christian Gentry, Maithreyi Gopalakrishnan, Henry C. Kapteyn, and Margaret M. Murnane, "Controlling Nonsequential Double Ionization in Two-Color Circularly Polarized Femtosecond Laser Fields," Phys. Rev. Lett. **117**(13), 133201 (2016).
44. S. Eckart, M. Richter, M. Kunitski, A. Hartung, J. Rist, K. Henrichs, N. Schlott, H. Kang, T. Bauer, H. Sann, L. Ph. H. Schmidt, M. Schöffler, T. Jahnke, and R. Dörner, "Nonsequential Double Ionization by Counterrotating Circularly Polarized Two-Color Laser Fields," Phys. Rev. Lett. **117**(13), 133202 (2016).
45. Y. Zhou, Q. Liao, Q. Zhang, W. Hong, and P. Lu, "Controlling nonsequential double ionization via two-color few-cycle pulses," Opt. Express **18**(2), 632–638 (2010).
46. H. Xie, M. Li, S. Luo, Y. Li, Y. Zhou, W. Cao, and P. Lu, "Energy-dependent angular shifts in the photoelectron momentum distribution for atoms in elliptically polarized laser pulses," Phys. Rev. A **96**(6), 063421 (2017).
47. A. Rudenko, Th. Ergler, K. Zrost, B. Feuerstein, V. L. B. de Jesus, C. D. Schröter, R. Moshammer, and J. Ullrich, "Intensity-dependent transitions between different pathways of strong-field double ionization," Phys. Rev. A **78**(1), 015403 (2008).
48. L. Fu, J. Liu, J. Chen, and S. Chen, "Classical collisional trajectories as the source of strong-field double ionization of helium in the knee regime," Phys. Rev. A **63**(4), 043416 (2001).
49. Z. Yuan, D. Ye, J. Liu, and L. Fu, "Inner-shell electron effects in strong-field double ionization of Xe," Phys. Rev. A **93**(6), 063409 (2016).
50. D. Ye, X. Liu, and J. Liu, "Classical Trajectory Diagnosis of a Fingerlike Pattern in the Correlated Electron Momentum Distribution in Strong Field Double Ionization of Helium," Phys. Rev. Lett. **101**(23), 233003 (2008).
51. Y. Zhou, Q. Liao, and P. Lu, "Asymmetric electron energy sharing in strong-field double ionization of helium," Phys. Rev. A **82**(5), 053402 (2010).
52. L. Fu, G. Xin, D. Ye, and J. Liu, "Recollision Dynamics and Phase Diagram for Nonsequential Double Ionization with Circularly Polarized Laser Fields," Phys. Rev. Lett. **108**(10), 103601 (2012).
53. M. V. Ammosov, N. B. Delone, and V. P. Krainov, "Tunnel Ionization Of Complex Atoms And Atomic Ions In Electromagnetic Field," Zh. Eksp. Teor. Fiz. **91**, 2008-2013 (1986).
54. N. B. Delone and V. P. Krainov, "Energy and angular electron spectra for the tunnel ionization of atoms by strong low-frequency radiation," J. Opt. Soc. Am. B **8**(6), 1207–1211 (1991).
55. S. Haan, Z. Smith, K. Shomsky, and P. Plantinga, "Anticorrelated electrons from weak recollisions in nonsequential double ionization," J. Phys. B **41**(21), 211002 (2008).
56. Y. Liu, D. Ye, J. Liu, A. Rudenko, S. Tschuch, M. Dürr, M. Siegel, U. Morgner, Q. Gong, R. Moshammer, and J. Ullrich, "Multiphoton double ionization of Ar and Ne close to threshold," Phys. Rev. Lett. **104**(17), 173002 (2010).
57. Y. Huismans, A. Rouzée, A. Gijsbertsen, J. H. Jungmann, A. S. Smolkowska, P. S. W. M. Logman, F. Lépine, C. Cauchy, S. Zamith, T. Marchenko, J. M. Bakker, G. Berden, B. Redlich, A. F. G. van der Meer, H. G. Muller, W. Vermin, K. J. Schafer, M. Spanner, M. Yu. Ivanov, O. Smirnova, D. Bauer, S. V. Popruzhenko and M. J. J. Vrakking, "Time-Resolved Holography with Photoelectrons," Science **331**(6013), 61–64 (2011).
58. M. Li, J.-W. Geng, M. Han, M.-M. Liu, L.-Y. Peng, Q. Gong, and Y. Liu, "Subcycle nonadiabatic strong-field tunneling ionization," Phys. Rev. A. **93**(1), 013402 (2016).
59. Q. Liao, Y. Li, M. Qin, and P. Lu, "Attosecond interference in strong-field nonsequential double ionization," Phys. Rev. A **96**(6), 063408 (2017).

1. Introduction

When exposed to a strong laser pulse, an atom or a molecule might be tunnel ionized with releasing an electron wave packet. The released electron is accelerated by the laser field, and it might be driven back to collide with the parent ion. Electron recollision is one of the most fundamental processes in strong-field physics [1], which can lead to high-harmonic generation (HHG) with electron recombination [2–7], high-order above-threshold ionization (HATI) [8, 9]

Optics EXPRESS

and laser-induced electron diffraction (LIED) [10–12] with elastic scattering, and nonsequential double ionization (NSDI) with inelastic scattering [13, 14]. In the NSDI process, the rescattering electron kicks out another electron, and thus the two electrons are highly correlated. The electron-electron correlation in NSDI has been studied for many years [15–24]. It has been shown that the electron-electron correlation is sensitive to the NSDI pathways, i.e., recollision impact direct ionization (RIDI) or recollision-excitation with subsequent field ionization (RESI) [25]. In addition, the multiple-recollision [26, 27] and multiple-returning-recollision [28, 29] trajectories may have a considerable contribution to the NSDI, which makes the electron-electron correlation in the NSDI more complex.

With the development of the laser technology, the control of electron wave packets by a strong field is achievable,which opens a new domain of attosecond science [30]. Several "knobs" are theoretically proposed and experimentally demonstrated to control the NSDI dynamics, such as the carrier envelope phase (CEP) of a few-cycle laser pulse [31–37] and the relative phase of a two-color laser pulse [38–45]. Liu *et al*. [33] have controlled the asymmetric ion emissions in the NSDI of Ar by changing the CEP of a few-cycle laser pulse. Subsequently, it was reported that the correlated electron momentum distribution also depends sensitively on the CEP of a few-cycle laser pulse [34–37]. Using two-color laser field can also achieve this manipulation. Zhou *et al*. [38] predicted that correlated or anticorrelated two-electron emissions can be switched by changing the relative phase of an orthogonally polarized laser field. This scheme controls the rescattering electron in the two-dimensional laser polarization plane, which was experimentally confirmed by Zhang *et al*. [41]. Up to now, most of the previous studies focused on the NSDI in the orthogonally polarized two-color laser fields [38–41] and circularly polarized two-color laser fields [42–44]. The NSDI in a few-cycle two-color laser pulse was studied by Zhou *etal*. [45]. The electron dynamics in the NSDI by a multicycle parallel polarized two-color laser field was not investigated before.

In this paper, we use a multicycle two-color laser pulse consisting of a strong 800-nm field and a weak parallel-polarized 400-nm field to control the correlated electron dynamics in strong-field NSDI of Ne. The weak 400-nm laser field is used to mildly streak the electron released by the strong 800-nm field. The recoil-ion momentum distributions from NSDI of Ne for different relative phases between the two-color components are measured by a cold target recoil ion momentum spectroscopy (COLTRIMS) system. We find that the peak of the ion momentum distribution shifts gradually with respect to the relative phase. We use a semiclassical ensemble model to reproduce the experimental data. The simulation agrees well with the measurement. Our results show that the energy sharing of the two electrons is extremely unequal at the instant of recollison. We further show that the recollision time can be mapped onto the ion momentum. The peak shift of the ion momentum distribution corresponds to the change of the vector potential at the recollision time. By tuning the relative phase between the two-color components, the recollision time can be controlled with attosecond precision.

2. Methods

2.1. Experiment

The laser pulse was generated by a Ti:sapphire femtosecond laser system (30 fs, 800-nm, 5 kHz repetition rate) and propagated through a 300-μm-thick β-barium borate(β-BBO) crystal for second harmonic generation (400-nm). After the BBO, the laser pulse consisted of both fundamental (800-nm) and second harmonic (400-nm) with orthogonal polarization. A dual wavelength wave plate was utilized to rotate the polarization direction of the fundamental component while keeping that of the second harmonic component unchanged. A wire grid polarizer combined with a second dual wavelength wave plate is used to adjust the intensity ratio of the two color field. The group delay between the two colors introduced by other optical elements and the window plate is compensated by a 2.6-mm-thick calcite plate. The relative

Optics EXPRESS

phase between the two-color components was controlled by a pair of glass wedges. The absolute value of the relative phase between the two-color components is calibrated by comparisons with the simulated singly-charged ion momentum distribution (see Fig. 1).

The two-color laser pulse is focused into the supersonic neon atomic beam with a parabolic mirror (f = 75 mm) to ionize the neon atoms. The focused spot diameter of the 800 nm component is about 7.64 μm and that of 400 nm component is about 3.82 μm. The energy for the whole pulse is about 25 μJ. The ion momentum was measured by a COLTRIMS system (see details in Ref. [46]). A weak uniform electric field of 1.2 V/cm is used across the spectrometer to guide the ion to the temporal and spatial-sensitive detectors(microchannel plate and delay-line anode). The resolution of the ion momentum along the laser polarization direction is about 0.1 atomic unit (a.u.). The momentum distribution of Ne^{2+} along the laser polarization direction exhibits an obvious double-peak structure, which allows us to calibrate the laser effective intensity by a comparison of the peak position with Ref. [47]. In the experiment, the effective intensity is calibrated to be $\sim 6.0 \times 10^{14}$ W/cm^2 for the 800-nm laser pulses, and the intensity ratio of two color components is estimated to be I_{800} :I_{400} = 40 : 1.

2.2. Numerical model

We use a semiclassical method to analyze the electron dynamics in the two-color laser fields. This model has been well developed for studying NSDI [48, 49]. It has been proved that the classical and semiclassical methods are very successful not only in interpreting the experimental results [50–52] but also in predicting new phenomena [38]. More importantly, the classical and semiclassical model have the advantage of back-tracing the classical trajectories, through which the underlying process can be intuitively presented [50]. Thus, in this paper we employ the two-dimensional semiclassical ensemble model [48] to study the electron dynamics of the NSDI by the two-color pulses.

In this semiclassical ensemble model, the ionization of the first electron from the bound state is treated by the tunneling ionization theory [53]. The tunneling electron (the first electron) has zero parallel velocity with respect to the laser polarization direction and a Gaussian transverse velocity distribution [54]. For the second electron, the initial position and momentum are depicted by the microcanonical distribution [48]. Then the subsequent evolution of the two electrons in the combined Coulomb and laser fields is described by the classical Newtonian equation (atomic units are used throughout until stated otherwise):

$$\frac{d^2\mathbf{r}_i}{dt^2} = -\nabla[V_{ne}(\mathbf{r}_i) + V_{ee}(\mathbf{r}_1, \mathbf{r}_2)] - \boldsymbol{\varepsilon}(t), \tag{1}$$

where the index i denotes the label of the two electrons, and $\mathbf{r}_i$ refers to the electron coordinates. $V_{ne}(\mathbf{r}_i) = -2/\sqrt{\mathbf{r}_i^2 + a^2}$ and $V_{ee}(\mathbf{r}_1, \mathbf{r}_2) = 1/\sqrt{(\mathbf{r}_1 - \mathbf{r}_2)^2 + b^2}$ are the Coulomb potentials between the nucleus and electrons, and between two electrons, respectively. The soft parameter a is set to 1.0 to speed up our calculation and b is set to 0.01 [50, 51, 55]. The electric field of the two-color pulse is written as $\boldsymbol{\varepsilon}(t) = f(t)[\varepsilon_\omega \cos(\omega t)\hat{\mathbf{x}} + \varepsilon_{2\omega} \cos(2\omega t + \phi)\hat{\mathbf{x}}]$ with ϕ the relative phase of the two colors, $\hat{\mathbf{x}}$ the laser polarization direction, ε_ω and $\varepsilon_{2\omega}$ the amplitudes of the 800-nm and 400-nm electric fields, respectively. $f(t)$ is the pulse envelope which is taken as

$$f(t) = \begin{cases} 1, & t \le 9\mathrm{T} \\ \cos^2(\dfrac{(t - 9\mathrm{T})\pi}{6\mathrm{T}}), & 9\mathrm{T} < \mathrm{t} \le 12\mathrm{T} \\ 0, & t > 12\mathrm{T} \end{cases} \tag{2}$$

where T is the optical period of the 800-nm field.

The weight of each trajectory is evaluated by $w(t_0, v^i_{\perp 0}) = w(t_0)w(v^i_{\perp 0})$ [48], in which

Optics EXPRESS

$$w(t_0) = \left(\frac{2(2I_{p1})^{1/2}}{|\varepsilon|}\right)^{\frac{2}{\sqrt{2I_{p1}}}-1} \exp\left(\frac{-2(2I_{p1})^{3/2}}{3|\varepsilon|}\right), \tag{3}$$

$$w(v_{\perp 0}^{i}) = \frac{1}{|\varepsilon|}\exp\left(-\frac{(v_{\perp 0}^{i})^2(2I_{p1})^{1/2}}{|\varepsilon|}\right). \tag{4}$$

$w(t_0)$ is the instantaneous tunneling probability and $w(v_{\perp 0}^{i})$ is the distribution of initial transverse velocity $v_{\perp 0}^{i}$. In our calculations, the first and second ionization potentials are chosen as $I_{p1} = 0.79$ a.u. and $I_{p2} = 1.5$ a.u., respectively, to match those of Ne. Several millions weighted classical two-electron trajectories are traced from the tunneling moment to the end of the pulse, resulting in more than 10^4 double ionization (DI) events for each relative phase. We define the recollision time as the instant corresponding to the shortest distance between the two electrons. The events with recollision energy lower than the first excitation energy of Ne^+, occur in our semiclassical simulation, are forbidden in the real experiment. To approximately take this effect into account in the semiclassical model [56], we have selected the DI trajectories for which the electron energy at the instant before the recollision (~0.03T before the recollision) is larger than the first excited state of Ne^+.

3. Results and discussions

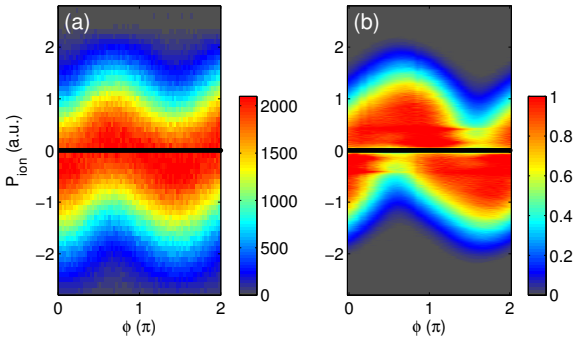

Fig. 1. Measured (a) and simulated (b) momentum distributions along the laser polarization direction of the Ne^+ ions with respect to the relative phase of the two-color laser field.

Figure 1 shows the measured and simulated momentum distributions along the laser polarization direction for the singly-charged Ne^+ ions with respect to the relative phase ϕ. One can see that both measured and simulated ion momenta strongly depend on the relative phase. Moreover, there are several stripe structures at near 0.5π and 1.5π in Fig. 1(b), which come from the strong Coulomb scattering effect when numerically solving the classical Newtonian equation [57, 58]. By comparing the simulated with measured momentum spectra, the absolute value of the relative phase between the two-color components in the experiment can be calibrated.

Figure 2(a) shows the measured Ne^{2+} momentum distribution along the laser polarization direction as a function of ϕ. The ion momentum corresponds to the sum of the two electron momenta by $p_{e_1} + p_{e_2} = -p_{ion}$. There are two characteristic features in the phase-dependent ion momentum distributions in Fig. 2(a). First, the distribution exhibits a pronounced asymmetric ion emission, which depends sensitively on the relative phase. This asymmetric ion emission is similar to the case in a few-cycle laser field [33, 37]. Second, the peak of the doubly charged ion momentum distribution shifts gradually with the relative phases. As guided by the black solid

Optics EXPRESS

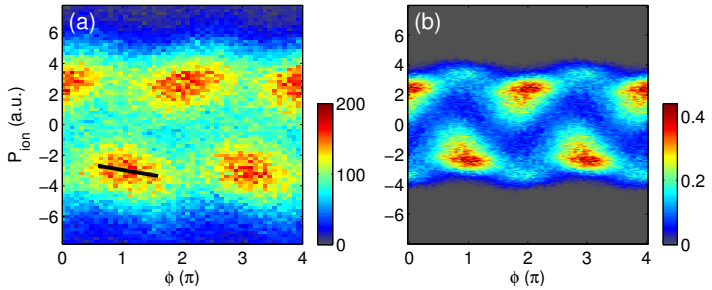

Fig. 2. Measured (a) and simulated (b) momentum distributions along the laser polarization direction of Ne^{2+} with respect to the relative phase of the two-color laser field. The black solid line in (a) shows the peak of the momentum distribution of Ne^{2+} at the relative phase from 0.5π to 1.5π. Note that the intensity averaging in the focal volume is not included in the simulation.

line, the peak shifts from -2.4 a.u. to -3.2 a.u. as the relative phase ϕ changes from 0.5π to 1.5π. The shift range is almost 0.6 a.u., which is larger than the maximal vector potential of the 400-nm laser field (~0.18 a.u.). This means that, though the intensity is quite low as compared with that of the 800-nm field, the 400-nm field plays a key role in the NSDI process. Those two features are well reproduced by the semiclassical model, as shown in Fig. 2(b). One can find the measured ion counts with p_{ion} between 4 a.u. and 6 a.u. (also -6 to -4 a.u.) are more than those in the simulated results. Two reasons are responsible for this difference. First, the simulated result is calculated with a single effective laser intensity without including the focal volume effect. Those measured high-energy ions might be generated by the high-intensity components in the laser focus. The other reason is that the effective laser intensity is a little underestimated by the simulation.

In light of the good agreement between the measured and simulated momentum distributions, we can use the semiclassical ensemble model to study the correlated electron dynamics in the two-color laser fields. In Figs. 3(c)-3(f), we show the correlated electron momentum distributions along the laser polarization direction calculated by the semiclassical ensemble model at the relative phases of $\phi = 1\pi$ [(c),(e)] and 1.5π [(d),(f)], corresponding to the most asymmetric and symmetric ion emissions in Fig. 2(a), respectively. The red dashed squares indicate the momentum of $2\sqrt{U_p}$. One can see that almost all electrons obtain final momenta smaller than $2\sqrt{U_p}$ in the two-color laser fields. The electric fields at the relative phases of 1π and 1.5π are shown in Figs. 3(a) and 3(b). For the relative phase $\phi = 1\pi$ [(c),(e)], the first electron is mainly released within [0.25T, 0.75T] and [1.25T, 1.75T] of Fig. 3(a) because the electric field strength within [0.25T, 0.75T] is larger than that within [0.75T,1.25T]. As a result, the yield in the first quadrant of the correlated electron momentum distribution is much larger than that in the third quadrant, thus the ion emission is asymmetric. At the relative phase $\phi = 1.5\pi$ [(d),(f)], the electric field strength is symmetric for the ionization times of [0.25T, 0.75T] and [0.75T,1.25T], thus the first electron is released with the same probabilities from both half cycles. Therefore, the yields in the first quadrant and in the third quadrant are nearly the same, leading to symmetric ion momentum distribution with respect to p_{ion}=0. The correlated electron momentum distribution for both relative phases exhibit clear V-shape structures, which are consistent with previous experiments [19, 20]. Back analysis of the electron trajectories reveals that almost of the double ionization events are caused by RIDI.

It is well known that the energy sharing ratio between the two electrons at the instant of the recollision is a crucial parameter in the RIDI process. This parameter describes how the recollision energy is shared by the two electrons and plays a significant role in the correlated electron momentum distributions [59] as well as the ion momentum distributions. To study the

Optics EXPRESS

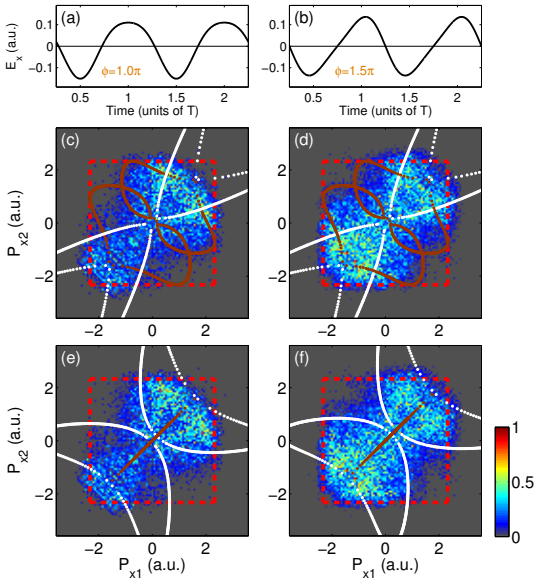

Fig. 3. Correlated electron momentum distributions along the laser polarization direction calculated by the semiclassical ensemble model using the two-color laser pulses at the relative phases $\phi = 1\pi$ [(c),(e)] and 1.5π [(d),(f)] and the corresponding laser electric fields [(a) and (b)]. The superimposed dots in (c)-(f) represent the results calculated by a classical one-dimensional recollision model. The energy sharing ratio between e_1 and e_2 at the instant of recollision is assumed to be 1 : 0 [(c),(d)] and 0.5 : 0.5 [(e),(f)]. The brown dots represent the final momenta of the first electron e_1 and the second electron e_2 in binary collision and the white dots represent the same in recoil collision. The red dashed squares indicate the $2\sqrt{U_p}$ cutoff momentum for tunneled electrons.

energy sharing in the two-color laser field, we use a simple one-dimensional classical recollision model with assuming different energy sharing ratios to obtain the correlated electron momentum distribution and compare it with the result from the semiclassical ensemble model. This simple recollision model has been used to study the formation of the V-shape structure before [20, 59], in which all Coulomb-field interactions among the two electrons and the parent ion are neglected. Briefly, the first electron is assumed to be born with zero momentum. When it is driven back by the laser field, a portion of the recollision energy is used to overcome the second ionization potential of Ne. The remaining energy is shared by the two electrons with different energy sharing ratios. After recollision, the direction of the second electron momentum is the same as that of the recolliding electron momentum before the recollision, while the direction of the first electron momentum is unchanged in a binary collision or reversed in a recoil collision [20, 59].

We show the results by the classical recollision model with the superimposed dots in Fig. 3. The energy sharing ratio between e_1 and e_2 is assumed to be 1 : 0 [Figs. 3(c) and 3(d)] and 0.5 : 0.5 [Figs. 3(e) and 3(f)], corresponding to extremely unequal and equal energy sharing, respectively. The brown dots represent the final momenta of the first electron e_1 and the second electron e_2 in binary collision and the white dots represent the same in recoil collision. Within the red dashed squares, the brown dots and the white dots are in good agreement with the structures calculated by the semiclassical ensemble model with the energy sharing ratio of 1:0. Nevertheless,the results with the energy sharing ratio of 0.5:0.5 for both binary and recoil collisions deviate largely with the semiclassical ensemble results. Thus, the energy sharing ratio of 1:0, i.e., the extremely unequal energy sharing, is favorable in this two-color laser field for Ne. This result validates the

Optics EXPRESS

asymmetric energy sharing rules in the high-intensity NSDI predicted by Ref. [51].

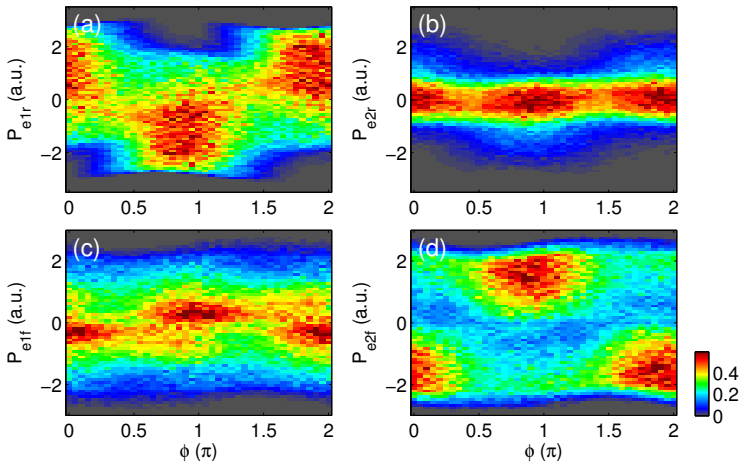

Fig. 4. The calculated momentum distributions along the laser polarization direction with respect to the relative phase after the recollision for the first electron e_1 (a) and the second electron e_2 (b), and the calculated final momentum distribution along the laser polarization direction of e_1 (c) and e_2 (d).

The extremely unequal energy sharing between the two electrons at the recollision time can also be revealed by the semiclassical ensemble model. Benefiting from this model, we can trace back the trajectories contributing to the NSDI. In Figs. 4(a) and 4(b), we show the momentum distribution almost 0.03T after the recollision time with respect to the relative phase for the first and second electrons, respectively, using the semiclassical ensemble method. One can see that the first-electron momenta show clear oscillations with respect to the relative phase with an amplitude up to 2 a.u., while the second electron momenta after the recollision are very close to zero for all relative phases ($|p_{e_2r}|$<0.4 a.u.). This also indicates that the energy sharing between the two electrons after the recollision is extremely unequal.

In Figs. 4(c) and 4(d), we further show the final momentum distribution with respect to the relative phase for e_1 and e_2, respectively. One can see that the case is reversed for the final electron momentum distribution, as compared with the electron momentum distribution after the recollision [Figs. 4(a) and 4(b)]. The first electron obtains a near-zero final momentum, whereas the second electron obtains a large final momentum along the laser polarization direction. This result can be well explained based on the extremely unequal energy sharing between the electrons. With neglecting the long-range Coulomb potential, the final momenta of the first and second electrons can be expressed as p_{e_1f}=v_r-$A(t_r)$ and p_{e_2f}=-$A(t_r)$, respectively. Here $A(t_r)$ is the vector potential at the recollision time t_r and v_r is the first-electron velocity after the recollision. For a high laser intensity, the recollision energy is much larger than the second ionization potential, thus the first-electron velocity after the recollision is approximately equal to the velocity before the recollision v_c, i.e., v_r=v_c=$A(t_r)$-$A(t_0)$, where t_0 is the ionization time for the first electron. Here we have assumed that the first electron is released with zero initial momentum. As a result, the final momenta for the two electrons can be approximately expressed as $p_{e_1f} \approx$ -$A(t_0)$ and $p_{e_2f} \approx$ -$A(t_r)$. Because the first electron is most likely released at the field maximum with $A(t_0)\approx 0$, the final momentum of the first electron is near to zero. The second electron can obtain a large final momentum depending on the recollision time.

Because the ion momentum is related to the sum of the two electron momenta, i.e., p_{ion}=-(p_{e_1f} + p_{e_2f}), we can obtain that $p_{ion} \approx A(t_r)$ for extremely unequal electron energy sharing after the

Optics EXPRESS

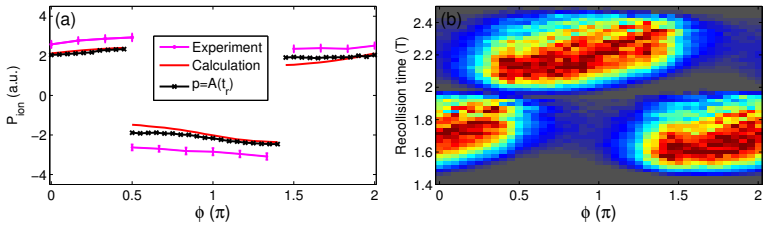

Fig. 5. (a) Comparison of the measured (mauve lines with dots) and simulated (red lines) peaks of the ion momentum distributions. The black solid lines with crosses show the vector potential at the instant of the recollision corresponding to the maximal ionization probability. Error bars are derived from the experiment based on Poissonian statistics and standard error propagation. (b) The distribution of the recollision time with respect to the relative phase.

recollision. As a result, the recollision time t_r can be mapped onto the final ion momentum. To demonstrate this point, we show the measured and simulated peaks of the ion momentum distributions with respect to the relative phase in Fig. 5(a). These peaks are obtained by a Gaussian fit of the ion momentum distribution in Fig. 2 for each relative phase. The vector potential at the instant of the recollision is also shown by the black solid lines with crosses. The vector potential at the instant of recollision agrees qualitatively with the measured and simulated peaks of the ion momentum distribution. The small difference between the simulation and the experiment may be due to an underestimation of the intensity of 800-nm component by the simulation. Ignoring this small difference, we can conclude that the recollision time is mapped onto the ion momentum. Though the 400-nm field is very weak, it can efficiently change the recollision time by tuning the relative phase between the two-color components. Because the vector potential at the recollision time is determined by both 400-nm and 800-nm fields, the ion momentum can be shifted with a range larger than the maximal vector potential of the 400-nm field with changing the relative phase. The peaks of the ion momentum distribution by the semiclassical ensemble model changes gradually from -1.8 a.u. to -2.4 a.u. when the relative phase is within $[0.5\pi, 1.5\pi]$. We can estimate that the recollision time is changed by almost 380 as according to $p_{ion} \approx A(t_r)$. This agrees well with Fig. 5(b), in which the recollision time is changed by about 400 as when the relative phase changes from 0.5π to 1.5π. The recollision time can be controlled with precision about 40 as when the relative phase is changed by 0.1π. Thus, we can control the recollision time with attosecond precision by tuning the relative phase of the two-color components.

4. Conclusion

In conclusion, we have measured the recoil-ion momentum distributions from nonsequential double ionization of Ne by multicycle two-color laser pulses consisting of a strong 800-nm field and a weak parallel-polarized 400-nm field. The measured ion momentum distribution shows a clear asymmetry in the emission direction with respect to the relative phase between the two-color components. This asymmetric emission comes from that the first electron in the NSDI is mainly released from one half cycle of the laser field. Moreover, the peak of the doubly charged ion momentum distribution shifts gradually with the relative phase. The shifted range is much larger than the maximal vector potential of the 400-nm laser field. We use a semiclassical ensemble model to reproduce the experimental result. Through analyzing the correlated electron momentum distribution, we found that the energy sharing of the two electrons is extremely unequal at the instant of recollison. We further show that the recollision time can be mapped onto the ion momentum and the shift of the ion momentum corresponds to the change of the vector potential at the recollision time. Though the 400-nm field is weak as compared with the

Optics EXPRESS

800-nm field, it can efficiently change the vector potential at the recollision time. Thus the peak of the ion momentum distribution is shifted with respect to the relative phase. By tuning the relative phase of the two-color components, we can control the recollision time with attosecond precision, which is significant for the study of time-resolved electron correlation in NSDI.

Funding

National Natural Science Foundation of China (NSFC) (11722432, 11674116, 11627809).